LA-UR-13-23365
Approved for public release; distribution is unlimited.

Title: Testing an Energy Dependent Albedo Capability for MCNP

Author(s): Fensin, Michael Lorne
McKinney, Alex B.
Hendricks, John S.

Intended for: America Nuclear Society Winter Meeting, 2013-11-10 (Washington, DC, District Of Columbia, United States)

Issued: 2013-05-08

Testing an Energy Dependent Albedo Capability for MCNP

M. L. Fensin, A. B. McKinney and J. S. Hendricks
Los Alamos National Laboratory, NEN-5, Los Alamos, NM 87545

INTRODUCTION

The objective of nuclear safeguards is to detect diversions of significant quantities of nuclear materials, and to deter such diversions through risk of early detection.[1] In order to provide the International Atomic Energy Agency (IAEA) with an instrument capable of directly measuring plutonium content in spent fuel assemblies, as well as the diversion of pins from these assemblies, the Next Generation Safeguard Initiative (NGSI) Spent Fuel project sponsored by the U.S Department of Energy (DOE) was started in March of 2009.[2] Goals of the project include development and/or calibration of Non-Destructive Assay (NDA) instruments using well-characterized or Working Standard assemblies. The definition of a Working Standard assembly is an assembly that applies NDA and/or Destructive Analysis (DA) data to a "base" simulation of the assembly to improve the accuracy of the simulation. One of the difficulties with developing a Working Standard has been simulating such a starting or "base" point for the assembly with limited operational data. The technique described in this paper establishes a path through which modifications to MCNP burnup simulations can be more easily applied in the creation of Working Standards.

To represent the vast amount of fuel expected to be measured by an IAEA inspector, multiple spent fuel libraries representing Pressurized Water Reactor (PWR) assemblies were developed using simulations with MCNPX 2.7.0[3] for characterizing detector response. These source terms include: (1) an infinitely reflected typical PWR fuel assembly, irradiated to varied burnups, with varied initial enrichments and cooling times in order to mimic the some of the typical PWR fuel assemblies found around the world;[4] and (2) a full core model, using a subset of the state-points from the first library, where only the assembly of interest is modeled in detail (treating all other neighboring assemblies as a single material of pins within each assembly) utilizing different shuffle patterns.[5] The first library used a reflected fuel assembly and axial homogenization. This setup was a crude approximation because in a real core the flux varies axially due to moderator density reduction from heat-up as well as radially due to the leakage and influx of neutrons from neighboring assemblies. The second library grouped pins as a single material within neighboring assemblies and axially homogenized the material, which lead to the same issues above; however, the second library did at least, to first order, address the effect of varying the neutron leakage by adjusting the boundary using fuel shuffling.

While a fuel assembly resides incore and operates at steady state power, the assembly sees a "critical spectrum" (i.e. energy dependent flux for a steady state system) that is dependent upon the fission and absorption properties of that assembly as well as neighboring assemblies that result in influx leakage. In an MCNP burnup calculation, each burn material region requires a finite amount of memory to store cross sections, nuclide densities and other MCNP bookkeeping arrays (i.e. identifying cell dependent properties). Even with the new MCNP memory reduction capability[6], a full core cannot be simulated with the detail necessary to capture the correct behavior of the radially and axially dependent influx leakage for a particular assembly in the core. Furthermore, a typical IAEA inspector may only be given an average assembly burnup; and therefore the one goal of the NGSI project is to provide a range of fuel assembly emission signals for an average burnup (i.e. change the boundary conditions to simulate many possible operating schemes).

Historically, when burning a single fuel assembly, the critical spectrum can be approximated using a buckling adjustment to the flux.[7, 8] The buckling adjustment uses properties of the fuel assembly and outgoing leakage to approximate the steady-state net leakage to renormalize the flux to mimic a "critical" spectrum. However, because net leakage really depends upon the neighboring fuel assemblies, this approximation is not necessarily accurate for all types of operating schemes (i.e. what if the assembly of interest is next to a fuel assembly with full rod insertion, or next to a control blade, or at a varied burnup, or using some other type of poison, or on the core periphery next to a reflector, etc.?). If the full core cannot be simulated, the next best idea is to apply (boundary-by-boundary) reasonably approximate boundary conditions using a separate albedo for each side of the truncated geometry. Using an energy integrated scalar albedo boundary to approximate a critical spectrum is not a new concept even in Monte Carlo depletion calculations.[9] The particular technique in Ref. 9 iteratively adjusts the incoming leakage until the modeled system is critical in order to get the "critical spectrum"; however, this method still relies only on knowledge of the outgoing leakage. In this paper, a new approach is tested to approximate boundary conditions, in Monte Carlo calculations, where a best representation of the boundary conditions is computed and applied to a truncated calculation. The procedure is as follows: (1) run a full core calculation

with "enough" detail; (2) tally on the energy dependent influx leakage to the assembly of interest; and (3) run a separate calculation using that influx leakage as and energy dependent albedo where the assembly is modeled in more explicit detail.

A new capability has been developed for MCNP6, which can utilize user-defined energy dependent albedos.[10] When a particle hits a designated reflective surface, the particle then can either be reflected using a designated amount of reflection or returned/killed using a designated albedo. The user sets the relative fraction of reflection or albedo as well as the weight of the returning particle. If an albedo is selected, the return probability (or weight if using implicit capture) is based upon a user specified magnitude, and the return energy is sampled from a user defined energy return function.

In this paper, this new capability is tested using a simple 3X3 matrix of fissile spheres contained in voided cubes, using various techniques to generate the albedo fraction and energy return function, to understand the limits in using this capability with various homogenization strategies.

METHOD

Several types of tests were completed comparing energy fidelity of the albedo and homogenization strategies for generating the albedo. The first test involved running a analog criticality calculation – 10,000 particles per cycle, with 100 settle cycles and 115 active cycles (to ensure the standard deviation of the worst case was less than 0.072% and averaged ~0.013%) – on a 3X3 matrix of fissile spheres contained within voided cubes, where the whole matrix was surrounded by a perfect absorber (Explicit 3X3). Energy dependent incoming surface currents, to the center cube, were then tallied at with 10, 50, 100, 500, 1000 and 1500 logarithmic energy bins from 1e-9 MeV to 30 MeV. The tallied incoming surface currents to the center region of the Explicit 3X3 were then used to generate the energy return functions. The reflection was set to zero, as these tests were only examining the use of the albedo alone; however, the albedo magnitude, used to sample whether a particle returned or not, was determined from either: (1) $k_{eff;}$ (2) total system leakage fraction; or (3) the ratio of the incoming to outgoing neutron current. These albedo boundaries were then used in a separate calculation containing only the center cube geometry (SCE). k_{eff} was compared between the Explicit 3X3 and SCE, with different energy binning strategies, to determine the minimum energy fidelity for the return function for use in constructing practical albedo boundaries.

The second test involved using a modified 3X3 matrix, where all outer cubes were homogenized, adjusting the density of fissile material in the homogenized regions by the ratio of the volume the sphere to the volume of the cube (Smear1 3X3). The third test was similar to the second, but homogenized all 9 cubes using the same procedure as the second test (Smear2 3X3). The same tallying/albedo file generation procedures as the first set of tests were followed (using the ratio of the incoming to outgoing currents method). Upon completion, the newly generated k_{eff} from the partial geometry (SC1 or SC2) was compared to the Explicit 3X3. The energy dependent lethargy of the Explicit 3X3 and was also compared to SCE, SC1 and SC2. For direct comparison, the flux tallies, in all the single cube cases, were normalized by the ratio of the fission neutron generation in the center region of the Explicit 3X3 as compared to the total fission neutron generation of the entire Explicit 3X3 (in reality a larger system power is known, and the relative power of a given region must be computed or estimated).

RESULTS

Table I presents the Δk_{eff} (SCE – Explicit 3X3) and summed relative error comparisons of the Explicit 3X3 to the SCE, for varied energy fidelities of the energy return function, where the albedo was set using: (1) k_{eff} [Keff]; (2) escape probability of the entire system (from the summary table) [Escape]; or (3) the ratio of the incoming to outgoing neutron current [Ratio]. The Ratio produced the best result (both 1000 and 1500 energy bins resulted in a Δk_{eff} ~0.00031) however, none of the cases resulted in a Δk_{eff} that was within 1σ. Both the escape probability of the entire system and k_{eff} are based on global behavior of the system and therefore using these quantities as a local albedo was not expected to be as accurate as using a local quantity such as entering and exiting currents for the region; nonetheless, it is interesting to note that: (1) using k_{eff} as an albedo always resulted in a lower k_{eff} in the single cube case by as much as ~2% (a fast spectrum system, with a smaller than bare critical radius and large streaming paths leads to more leakage than multiplication); and (2) using the system escape probability always resulted in a higher k_{eff} (the total system escape probability will be higher than the center region as the out spheres bordered a perfect absorber and reaching that perfect absorber was considered escape).

Table I. Δk_{eff}, and summed relative error, of the Explicit 3X3 as compared to SCE, for varied albedo magnitudes and energy fidelities of the energy return functions.

Energy	Keff	RE	Escape	RE	Ratio	RE
10	-0.537%	0.046%	3.127%	0.073%	1.933%	0.052%
50	-1.974%	0.027%	1.116%	0.026%	0.106%	0.028%
100	-2.004%	0.024%	1.107%	0.025%	0.056%	0.025%
500	-2.011%	0.025%	1.086%	0.026%	0.042%	0.026%
1000	-2.036%	0.023%	1.062%	0.027%	0.031%	0.027%
1500	-2.013%	0.024%	1.107%	0.025%	0.031%	0.025%

A 10,000 energy bin case was also completed that resulted in a Δk_{eff} = 0.015% with a summed relative error of 0.018% (falling within 1σ). As more energy bins are tallied for the energy return function, more particles must be run to ensure energy return function's energy bins have converged; therefore for the same finite amount of sampled particles, a higher fidelity energy bin structure will be noisier than a coarser tally structure. The energy return functions represent the integral amount of particles within a particular energy bin, and are set as renormalized probability density functions when sampling the return energy; therefore to compare noisiness of this function as a function of energy fidelity, Fig. 1 displays the energy return function divided by the energy bin width for 10, 100 and 1000 energy bin fidelity (the return function is not weighted with albedo magnitude). The noisiness in Fig. 1 was related to: (1) resonances (scatter, capture and fission) that result in a density of neutrons about a particular energy bin; and (2) the fact that a particular energy bin may not have converged (i.e. large relative error). Therefore the fact that the 1000 bin case fell outside of 1σ and 10,000 bin case fell within 1σ may either be related to statistics or better representation of a resonance.

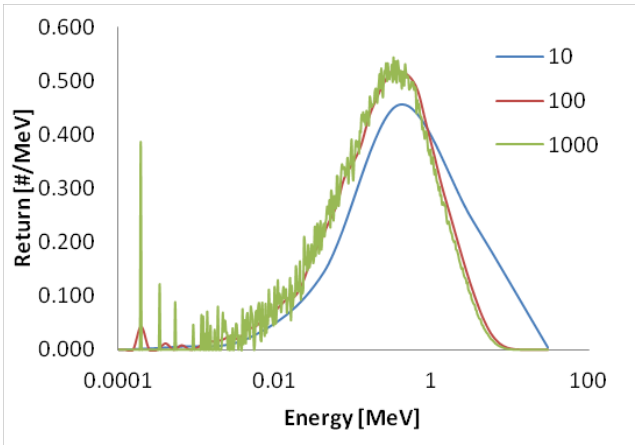

Fig 1. Energy return function for 10, 100 and 1000 energy bin fidelity (1e-9 -- 30 MeV).

Table II. Δk_{eff}, and summed relative error, of the Explicit 3X3 as compared to SC1, for varied energy fidelities of the energy return function and albedo magnitude.

Energy	Keff	RE	Escape	RE	Ratio	RE
10	-2.081%	0.038%	3.964%	0.062%	-6.330%	0.026%
50	-3.173%	0.025%	1.832%	0.025%	-6.804%	0.022%
100	-3.183%	0.025%	1.768%	0.026%	-6.803%	0.023%
500	-3.206%	0.025%	1.776%	0.026%	-6.795%	0.023%
1000	-3.207%	0.025%	1.777%	0.026%	-6.804%	0.024%
1500	-3.222%	0.023%	1.753%	0.027%	-6.833%	0.023%

Table II and Table III present the Δk_{eff}, and summed relative error comparisons of the Explicit 3X3 to either SC1 or SC2, where the albedos were generated from Smear1 3X3 or Smear2 3X3.

Examining Table II, setting the albedo for the SC1 based on the ratio of the currents from Smear1 3X3 resulted in an enormous, >6%, Δk_{eff}. However, the Smear1 3X3 boundary, when applied to SC1, produced a k_{eff} that was roughly the same as the Smear1 3X3. The fission-to-capture ratios, for the center region, of both the Explicit 3X3 and Smear1 3X3 cases were ~10. Therefore the enormous Δk_{eff} of SC1 was due to the fact that by homogenizing the outer cubes there was less streaming escape and more reflective scatter. In fact, the albedo magnitude generated by the Smear1 3X3 was 3.6 times less than the Explicit 3X3.

Table III. Δk_{eff}, and summed relative error, of the Explicit 3X3 as compared to SC2, for varied energy fidelities of the energy return function and albedo magnitude.

Energy	Keff	RE	Escape	RE	Ratio	RE
10	-4.902%	0.033%	6.458%	0.084%	2.744%	0.063%
50	-5.644%	0.026%	3.755%	0.028%	0.698%	0.028%
100	-5.643%	0.024%	3.712%	0.027%	0.672%	0.026%
500	-5.677%	0.025%	3.717%	0.027%	0.644%	0.028%
1000	-5.650%	0.023%	3.674%	0.028%	0.632%	0.027%
1500	-5.656%	0.022%	3.668%	0.028%	0.644%	0.026%

The Smear2 3X3 contained homogenization of all cubes. As a result of this homogenization scheme, the outer cubes as compared to the inner cube both did not contain any direct streaming paths. The Δk_{eff} was much closer to the Explicit 3X3, ~0.64%; this is still significantly different. The fission-to-capture ratio of the center region of Smear2 3X3 was also ~10, and the albedo of the Smear2 3X3 was ~2% larger than the Explicit 3X3.

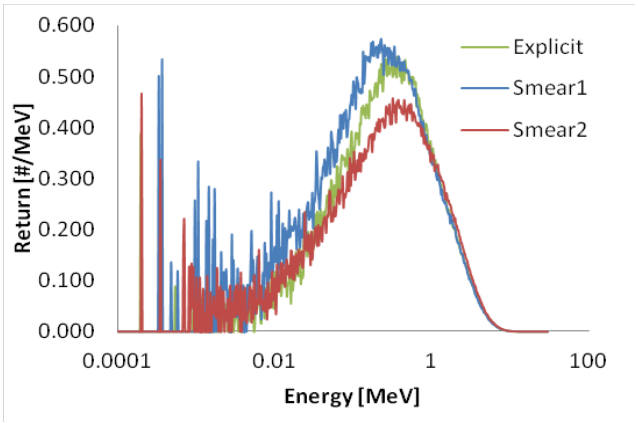

Fig 2. Energy return function for the 1000 energy bin (1e-9 -- 30 MeV) 3X3 using Explicit, Smear1 and Smear2.

Fig. 2 displays the energy return function of the 1000 energy bin case for each 3X3 homogenization strategy (the return function was not weighted with albedo magnitude). Unlike Fig. 1, the magnitude of the albedo of

each of these cases was different (Smear2 3X3 > Explicit 3X3 > Smear1 3X3). Because the energy return functions were not weighted with the albedo, only the relative structure of the curves was useful. Ignoring the total magnitude of each curve, but examining the relative peak to trough, Smear1 3X3 was much more peaked between 100 keV – 1 MeV and the width of the peak was much greater than both the Explicit 3X3 and Smear2 3X3. Therefore, to first order, the increased density of particles returned within the 100 keV – 1 MeV range for Smear1 3X3, as opposed to more thermal or high energies (which have larger fission-to-capture ratio than the resonance regime), resulted in more resonance capture as opposed to fission leading to a reduced k_{eff}. Likewise, the decreased density of particles returned within the 100 keV – 1 MeV for Smear2 3X3 resulted in less resonance capture as opposed to fission leading to an increased k_{eff}. To be complete, these effects also must be weighted with the changes in the physical geometry that affect leakage; nonetheless, to first order, these effects give insight into how symmetry between cells results in similar ratios of the incoming to outgoing current.

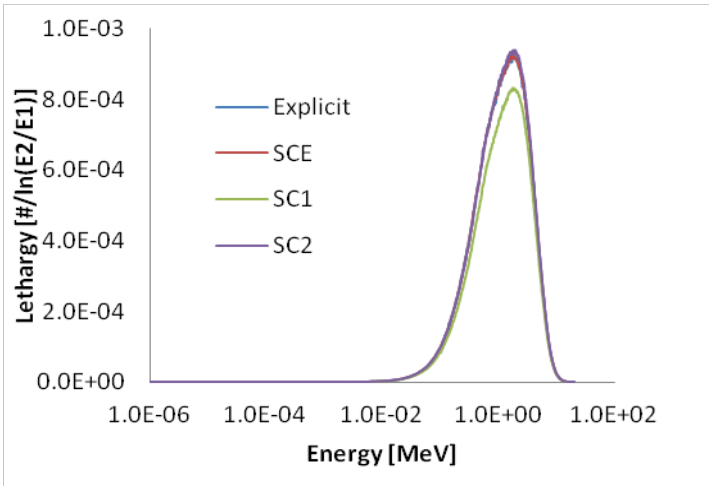

Fig 3. Energy dependent lethargy for Explicit 3X3, SCE, SC1 and SC2.

Since k_{eff} is an integral quantity composed of a balance of interaction rates, the magnitude and shape of the energy dependent flux was also examined. Fig. 3 plots the energy dependent lethargy (1eV – 20 MeV with 1000 logarithmic intervals) for the: (1) center region of the Explicit 3X3; (2) SCE, 1000 energy bin Ratio method; (3) SC1, 1000 energy bin Ratio method; and (4) SC2, 1000 energy bin Ratio method. The energy integrated flux for the center region of the Smear1 3X3 is ~2.22 times higher than the Explicit 3X3, and the Smear2 3X3 is 3.5% lower than the Explicit 3X3; however, for Fig 3, all curves (Except the Explicit 3X3 matrix) are renormalized based on the relative fission rate of the center region of the Explicit 3X3. This illustrates an important point. If each case is normalized by the corresponding relative fission rate, for each separate geometry type (explicit and homogenized), the SC1 flux would be significantly higher but the SC2 flux would only be slightly lower. As a result, comparing SCE to SC1 (SCE/SC2-1) (using the specific normalizations generated from the Explicit 3X3, Smear1 3X3 and Smear2 3X3) capture was 1.82 times higher, fission was 1.85 times higher and fission neutron production was 1.86 times higher. Using the same normalization for all three cases, capture was only 12.6% lower, fission was only 11.4% lower and fission neutron production was only 11.3% lower (as compared to the Explicit 3X3). Comparing SCE to SC2 (SCE/SC2-1) (using the specific normalizations generated from the Explicit 3X3, Smear1 3X3 and Smear2 3X3) capture was 3.92% higher, fission was 4.32% higher and fission neutron production 4.36% higher. Using the same normalization for all three cases, capture, fission and fission neutron production were all within >1% (as compared to the Explicit 3X3).

CONCLUSIONS

The new energy dependent albedo boundary capability is a promising new solution for imitating the properties of a full geometry, using only a partial geometry. This technique could therefore be used to replace a buckling search as this technique can better represent effects from asymmetric boundaries. These simple tests focus on the ability to compute k_{eff} and lethargy for a cropped geometry using only the explicit geometry of the cropped section with proper boundary conditions to approximate the inflow leakage. The albedo is related to the ratio of inflow to outflow leakage at the boundary. The accuracy of the results are highly dependent on the fidelity of the energy return function and magnitude of the albedo (1000 bins seems to be good enough); and therefore future work will focus on trying to map the necessary fidelity of the return function to tractable properties of the geometry (i.e. cross section resonances, etc.). The tests using the explicit geometry verify that the capability is functioning properly, and that the ratio of the fission rate of the center region to total fission rate of the system is the correct normalization for the flux.

The tests using two different homogenization strategies do give insight into what boundary approximations affect the final solution the most: (1) a boundary generated from a geometry (cell-to-cell) that has asymmetry results in significantly different transport (i.e. significantly changing the non-leakage probability significantly changes the transport) as compared to a boundary generated from a geometry that has symmetry, resulting in significantly different k_{eff} (and fluxes); (2) a boundary generated from a geometry that has a similar symmetry as compared to a base geometry, even if the total streaming is significantly different, results in a k_{eff} that is closer to the true value than (1); and (3) determining the relative power is important as this

quantity is used to directly normalize the flux of the cropped geometry. Using the actual relative power to normalize the flux for SC2 resulted in capture, fission and fission neutron production that was within 1%. Since major fission product yields are usually not known to within 10% and actinide production is usually not known to within a few percent, the 1% difference in reaction rates may be tolerable for large scale burnup simulations.

ACKNOWLEDGMENTS

The authors would like to acknowledge the support of the Next Generation Safeguards Initiative (NGSI), Office of Nonproliferation and International Security (NIS), National Nuclear Security Administration (NNSA).

REFERENCES

1. IAEA, INFCIRC/153 (Corrected), "The Structure and Content of Agreements Between the Agency and States Required in Connection with the Treaty on the Non-Proliferation of Nuclear Weapons," *International Atomic Energy Agency*, Vienna, Austria (1972).
2. S. J. TOBIN, et. al., "Determination of Plutonium Content in Spent Fuel with Nondestructive Assay," *Trans. INMM*, July 12-16, Tucson, AZ, (2009).
3. D. B. PELOWITZ, editor," MCNPX User's Manual Version 2.7.0," *LA-CP-11-00438* (2011).
4. M. L. FENSIN, S. J. Tobin, N. P. Sandoval, S. J. Thompson, M. T. Swinhoe, "A Monte Carlo Linked Depletion Spent Fuel Library for Assessing Varied Nondestructive Assay Techniques for Nuclear Safeguards," *ANFM IV*, Hilton Head Island, South Carolina (2009).
5. JACK D. GALLOWAY, Holly R. Trellue, Michael L. Fensin, and Bryan L. Broadhead, "Design and Description of the NGSI Spent Fuel Library with Emphasis on the Passive Gamma Signal," *Journal of Nuclear Materials Management*, **40**, issue 3, pg 25-36 (April 2012).
6. MICHAEL L. FENSIN, Michael R. James, John S. Hendricks, John T. Goorley, "The New MCNPX Depletion Capability," *International Congress on the Advancements in Nuclear Power Plants*, Chicago, IL (2012).
7. A. FODERARO, "An Iteration Method for the Specification of Multigroup Bucklings," *Nuclear Science and Engineering*, **6**, pg 514-525 (1959).
8. D. KNOTT, E. Wehlage, "Description of the LANCER02 Lattice Physics Code for Single-Assembly and Multibundle Analysis," *Nuclear Science and Engineering*, **155**, pp. 331-354 (2007).
9. S. YUN and N. Z. Cho, "Monte Carlo Depletion Under Leakage-Corrected Critical Spectrum via Albedo Search," *Nuclear Engineering and Technology*, **42**, pg 271-278 (June 2010).
10. J. S. HENDRICKS, S. J. Tobin, "NGSI MCNPX Extensions to MCNPX 270," *LA-UR-12-00133* (2012).